ISSN 1560-3547, Regular and Chaotic Dynamics, 2015, Vol. 20, No. 1, pp. 37–48. © Pleiades Publishing, Ltd., 2015.

Dynamics of the Finite-dimensional Kuramoto Model: Global and Cluster Synchronization

Vladimir N. Belykh*, Valentin S. Petrov, and Grigory V. Osipov*****

Department of Control Theory, Nizhny Novgorod University,
ul. Gagarina 23, Nizhny Novgorod, 603950 Russia

Received November 11, 2014; accepted December 24, 2014

Abstract—Synchronization phenomena in networks of globally coupled non-identical oscillators have been one of the key problems in nonlinear dynamics over the years. The main model used within this framework is the Kuramoto model. This model shows three main types of behavior: global synchronization, cluster synchronization including chimera states and totally incoherent behavior. We present new sufficient conditions for phase synchronization and conditions for an asynchronous mode in the finite-size Kuramoto model. In order to find these conditions for constant and time varying frequency mismatch, we propose a simple method of comparison which allows one to obtain an explicit estimate of the phase synchronization range. Theoretical results are supported by numerical simulations.

MSC2010 numbers: 34C25, 34C28, 34C46, 37C75

DOI: 10.1134/S1560354715010037

Keywords: phase oscillators, Kuramoto model, global synchronization, existence and stability conditions, asynchronous mode

1. INTRODUCTION

The formation of collective behavior in large ensembles or networks of coupled non-identical oscillatory elements is one of the oldest problem in the study of dynamical systems. Nevertheless, it is an actually challenging field for a theoretical understanding as well as for applications in various disciplines, ranging from physics, chemistry, earth sciences via biology and neuroscience to engineering, business and social sciences. Due to the large number of effective degrees of freedom in spatially extended systems, a rich variety of spatiotemporal regimes is observed. Three main types of collective behavior are distinguished: (i) a fully incoherent state or highly developed spatiotemporal disorder; (ii) partially coherent states, where some of the participants in the network behave in some common rhythm; (iii) a fully coherent state or a regime of globally synchronized elements. The basic phenomenon of these structure formations is synchronization, i.e., regime of coherent activity, which is universal in many dynamical systems and can be understood from the analysis of common models of oscillatory networks.

Cooperative phenomena in ensembles of globally (mean-field) coupled phase equations were studied first by Winfree [1]. He mathematically reduced the problem of mutual synchronization to that of a collective behavior in an ensemble of coupled *phase oscillators*. He showed that such oscillator ensembles could demonstrate a temporal analog of a thermodynamic phase transition: with the increase of the coupling a group of oscillators suddenly becomes synchronized. By using perturbation methods of averaging, Kuramoto [2, 3] obtained a model of weakly *globally* coupled, nearly identical limit-cycle oscillators. The governing system of this model are first-order dynamical equations with sinusoidal coupling function. This paradigmatic model appears in many applications in science and engineering. Examples are cells in the heart [4], Hodgkin – Huxley neurons [5], central pattern generator for animal locomotion [6], coupled Josephson junctions [7], rhythmic applause [8],

*E-mail: belykh@unn.ru
**E-mail: valentin.s.petrov@gmail.com
***E-mail: osipov@vmk.unn.ru

pedestrian crowd synchrony on London's Millennium bridge [9], semiconductor laser arrays [10], microwave oscillator arrays [11] etc. For other examples, see [12].

Most results for the Kuramoto model are obtained in the case of infinite dimension (for review, see [12–14]). In the finite-dimensional case various conditions of the synchronization band have been proposed [12, 15–18]. In this paper, we present new sufficient conditions for phase synchronization and conditions for an asynchronized mode in the finite-size Kuramoto model.

2. THEORETICAL ESTIMATES

The well-known Kuramoto model [3] of phase oscillators has the form

$$\dot{\phi}_i = \omega_i + \xi_i(t) + \frac{K}{N}\sum_{j=1}^{N}\sin(\phi_j - \phi_i), \quad i = \overline{1,N}, \tag{2.1}$$

where ϕ_i are phases, ω_i are natural frequencies, $\xi_i(t)$ is external noise, K is coupling, and N is the number of oscillators.

The basic tool in studying the model (2.1) is the "mean field" approach. That is, the substitution

$$re^{j(\psi-\phi_i)} = \frac{1}{N}\sum_{k=1}^{N} e^{j(\phi_k-\phi_i)}, \tag{2.2}$$

and the right-hand side in (2.1) is changed such that

$$\dot{\phi}_i = \omega_i + \xi_i(t) + Kr\sin(\psi - \phi_i), \quad i = \overline{1,N}. \tag{2.3}$$

This change is valid when r and ψ in (2.2) do not depend on ϕ_k, and this is true for $N \to \infty$. The latter constitutes the "mean field" in "all-to-all" configuration of phase oscillators (2.1).

For the finite number N the order parameters r and ϕ can be written in the form

$$\begin{gathered} r = \sqrt{\left(\frac{1}{N}\sum_{k=1}^{N}\sin\phi_k\right)^2 + \left(\frac{1}{N}\sum_{k=1}^{N}\cos\phi_k\right)^2} \leqslant 1, \\ \psi = \arctan\frac{\sum_{k=1}^{N}\sin\phi_k}{\sum_{k=1}^{N}\cos\phi_k} \end{gathered} \tag{2.4}$$

and straightforward conclusions about synchronization for the finite number N via (2.4) cannot be drawn.

The main goal of this paper is to present sufficient conditions for phase synchronization in the Kuramoto model for any finite number of phase oscillators.

2.1. Properties of the Kuramoto Model

1. Consider the Kuramoto equations for homogenous perturbation $\xi_i(t) \equiv \xi(t)$,

$$\dot{\phi}_i = \omega_i + \xi(t) + \frac{1}{N}\sum_{j=1}^{N}\sin(\phi_j - \phi_i), \quad i = \overline{1,N}, \tag{2.5}$$

where $\xi(t)$ is an arbitrary continuous function. The change of variables $\phi_i = \tilde{\phi}_i + \int \xi(t)dt$ reduces the system (2.5) to the original unperturbed system. Hence, the Kuramoto model admits

- well-known transition to the rotation mode when $\xi(t) = \Omega = \text{const}$, that is why one considers $\sum_{i=1}^{N}\omega_i = 0$
- simultaneous escape of all phases, when, for instance, $\xi(t) = e^t$

- effects of additive common noise are equivalent to additive perturbation of the stationary process of the unperturbed system.

2. The unperturbed Kuramoto system has the invariant foliation $\sum_{i=1}^{N}\phi_i = \text{const}$, since $\sum_{i=1}^{N}\dot{\phi}_i = \sum_{i=1}^{N}\omega_i$. This implies that the Kuramoto model is an excessive system of ODE and cannot have any asymptotically stable states: the coordinate "u" along the vector $(1, 1, \ldots, 1)$ satisfies the equation $\dot{u} = 0$.

2.2. Phase Difference Equations

We rewrite the system (2.1) in order to exclude one equation. We choose the first oscillator as a leading one and introduce new variables and new parameters:

$$\Theta_j = \phi_j - \phi_1, \Delta_j = \omega_j - \omega_1 + \xi_j - \xi_1, \quad j = \overline{1, N}, \tag{2.6}$$

where Θ_j is the phase difference and Δ_j is the frequency mismatch of j's and leading oscillators.

Proposition. *The system* (2.1) *can be rewritten as*

$$\dot{\Theta}_i = \Delta_i - KR\sin\Theta_i, \quad i = \overline{1, N}, \tag{2.7}$$

where $R = \frac{1}{N}\sum_{j=1}^{N}\left(\frac{\cos(\Theta_i/2-\Theta_j)}{\cos(\Theta_i/2)}\right)$.

Note that the trivial first equation $\dot{\Theta}_1 = 0, \Theta_1 = 0, \Delta_1 = 0$ reduces the dimension of the system due to the existence of invariant foliation, and the function R can be referred to as a new "order parameter".

Indeed, introducing phase differences and frequency mismatch (2.6), we rewrite the system in the form

$$\begin{aligned}\dot{\Theta}_i &= \omega_i + \frac{K}{N}(\sin(\Theta_1 - \Theta_i) + \sin(\Theta_2 - \Theta_i) + \cdots + \sin(\Theta_n - \Theta_i)),\\ \dot{\Theta}_1 &= \omega_1 + \frac{K}{N}(\sin\Theta_1 + \sin\Theta_2 + \cdots + \sin\Theta_n),\end{aligned} \tag{2.8}$$

from which we obtain equations for the new variables

$$\dot{\Theta}_i = \Delta_i - \frac{K}{N}\sum_{j=1}^{N}\left(\sin\Theta_j - \sin(\Theta_j - \Theta_i)\right). \tag{2.9}$$

Using the formula $\sin\Theta_j - \sin(\Theta_j - \Theta_i) = 2\sin\frac{\Theta_i}{2}\cos(\frac{\Theta_i}{2} - \Theta_j)$, we come to the final form of the system

$$\dot{\Theta}_i = \Delta_i - K\left[\frac{2}{N}\sum_{j=1}^{N}\cos\left(\frac{\Theta_i}{2} - \Theta_j\right)\right]\sin\frac{\Theta_i}{2}, \tag{2.10}$$

which is equivalent to the system (2.7).

3. DYNAMICS OF THE KURAMOTO SYSTEM

3.1. Identical Oscillators

In this trivial case the frequency differences $\Delta_i = 0$, Eq. (2.7) takes the form

$$\dot{\Theta}_i = -K\frac{1}{N}\sum_{j=1}^{N}\left(\frac{\cos(\Theta_i/2 - \Theta_j)}{\cos(\Theta_i/2)}\right)\sin\Theta_i, \quad i = \overline{1, N}. \tag{3.1}$$

The zero equilibrium point O ($\Theta_i = 0$, $i = \overline{1,N}$) is exponentially stable, since the variational equation is $\dot{u}_i = -Ku_i$. The basin of equilibrium O is

$$|\Theta_i| < \frac{\pi}{3}, \quad i = \overline{1,N}. \tag{3.2}$$

It follows from the Lyapunov function

$$V = \sum_{i=1}^{N}(1 - \cos\Theta_i), \tag{3.3}$$

which derivative with respect to (3.1) is

$$\dot{V} = -K\frac{1}{N}\sum_{j=1}^{N}\left(\frac{\cos(\Theta_i/2 - \Theta_j)}{\cos(\Theta_i/2)}\right)\sin^2\Theta_i < 0 \quad \text{for} \quad |\Theta_i| < \frac{\pi}{3}, \Theta_i \neq 0, i = \overline{1,N}.$$

3.2. Equal Frequency Differences $\Delta_i = \Delta = \text{const}$ (the Differences Against the Leader are Equal)

Equation (2.7) takes the form

$$\dot{\Theta}_i = \Delta - KR\sin\Theta_i. \tag{3.4}$$

This system has a 1D invariant manifold $J = \{\Theta_i = \Theta,\ i = \overline{1,N}\}$. Due to the equality $R|_J = 1$ the dynamics in J is given by the equation

$$\dot{\Theta} = \Delta - K\sin\Theta \tag{3.5}$$

and $|\Delta| < K$ is the condition of stable synchrony in J ($\Theta^* = \arcsin\frac{\Delta}{K}$). The stability transversal to J can be derived using variational equations.

4. SUFFICIENT CONDITION FOR PHASE SYNCHRONIZATION OF THE KURAMOTO OSCILLATORS

Consider for simplicity the case of different constant values of frequency mismatches in (2.7).

The phase synchronization of oscillators is defined as a steady state $\Theta_i^*(t)$, $i = \overline{1,N}$ such that

$$|\Theta_i^*| \leqslant \alpha, \quad i = \overline{1,N}, \tag{4.1}$$

where α is a parameter of phase mismatch in (2.1).

The function R in (2.7) satisfies the condition

$$\frac{1}{N}\sum_{j=1}^{N}\left(\frac{\cos(\Theta_i/2 - \Theta_j)}{\cos(\Theta_i/2)}\right) > 0 \quad \text{for} \quad |\Theta_i| < \frac{\pi}{3}, \quad i = \overline{1,N}. \tag{4.2}$$

Now we choose some value of α in (4.1), $\alpha < \frac{\pi}{3}$ and obtain the bounds

$$\cos\frac{3\alpha}{2}\cos^{-1}\frac{\Theta_i}{2} < R < \cos^{-1}\frac{\Theta_i}{2}. \tag{4.3}$$

Using (4.3), we introduce two auxiliary systems

$$\begin{aligned} \dot{\Theta}_i &= \Delta_i - 2K\sin\frac{\Theta_i}{2}, \quad i = \overline{1,N}, \\ \dot{\Theta}_i &= \Delta_i - 2K\cos\frac{3\alpha}{2}\sin\frac{\Theta_i}{2}, \quad i = \overline{1,N} \end{aligned} \tag{4.4}$$

defined in the compact $C = \{\Theta|\ |\Theta_i| < \alpha,\ i = \overline{1,N}\}$.

4.1. Comparison Principle

In order to obtain sufficient conditions for phase synchronization, we use the comparison principle, which is formulated as follows. Given a system

$$\dot{x} = F(x), \quad x = (x_1, \ldots, x_n), \quad F = (F_1, \ldots, F_n), \tag{4.5}$$

and a compact $C = \{x|\ |x_i| \leqslant \alpha,\ i = \overline{1,n}\}$, we introduce the comparison systems

$$\begin{gathered} \dot{x}_i = F_i^+(x_i), \quad i = \overline{1,n}, \\ \dot{x}_i = F_i^-(x_i), \quad i = \overline{1,n}, \\ |x_i| \leqslant \alpha, \end{gathered} \tag{4.6}$$

where $F_i^+ = \sup\limits_{\substack{|x_j|\leqslant\alpha \\ j\neq i}} F_i(x_1, \ldots, x_n)$, $F_i^- = \inf\limits_{\substack{|x_j|\leqslant\alpha \\ j\neq i}} F_i(x_1, \ldots, x_n)$.

Assumption 1. *Assume that $F_i^{\pm}(x_i)$ are continuous functions such that each of them has a unique zero at the interval $[-\alpha, \alpha]$, $x_i = \beta_i^{\pm} \in [-\alpha, \alpha]$, and $F_i^{\pm}(x_i) \cdot (x_i - \beta_i^{\pm}) < 0$, $x_i \in [-\alpha, \alpha]$, $x_i \neq \beta_i^{\pm}$.*

Due to these conditions the points $\beta_i^{\pm}$ are stable equilibrium points of the comparison system (4.6). Since $F_i^+ \geqslant F_i^-$, $x_i \in [-\alpha, \alpha]$, we have $\beta_i^- \leqslant \beta_i^+$, and we introduce a compact $C_\beta = \{x|\beta_i^- \leqslant x_i \leqslant \beta_i^+,\ i = 1, \ldots, n\}$, $C_\beta \subset C$.

Theorem 1. *Let the Assumption* 1 *hold. Then the system* (2.1) *has an attractor A lying in the compact C_β, and the compact C lies in the basin of the attractor A, $A \subset C_\beta \subset C$.*

Proof. Consider the directing Lyapunov function

$$V = \sum_{i=1}^{n} \left| x_i - \frac{\beta_i^+ - \beta_i^-}{2} \right| \tag{4.7}$$

in the domain $C \backslash C_\beta$. Its derivative with respect to the system (4.5) is

$$\dot{V} = \sum \Phi_i, \tag{4.8}$$

where

$$\Phi_i = \begin{cases} F_i, & \text{if } \ x_i \in [\beta_i^+, \alpha], \\ -F_i, & \text{if } \ x_i \in [-\alpha, \beta_i^-]. \end{cases} \tag{4.9}$$

Since the inequalities

$$F_i \leqslant F_i^+ < 0,\ x_i \in [\beta_i^+, \alpha],\ -F_i < -F_i^- < 0,\ x_i \in [-\alpha, \beta_i^-] \tag{4.10}$$

hold, $\dot{V} < 0$ for $x \in C \backslash C_\beta$. Hence any trajectory of the system (4.5) starting at the initial point $x_0 \in C \backslash C_\beta$ enters the compact C_β, and C_β contains a limiting set – attractor A. □

Corollary 1. *There exists at least one equilibrium point of the system* (4.5) *in the compact C_β. This statement follows from the Brouwer fixed point theorem for the map $\eta : x \to (x + \tau F(x))$, where $\tau > 0$ is small enough, since $\eta C_\beta \subset C_\beta$.*

Corollary 2. *The theorem is true in the case when the system* (4.5) *is nonautonomous. Here the functions in* (4.6) *should be replaced with $\tilde{F}_i^+ = \sup_{t\in R^1} F_i^+$, $\tilde{F}_i^- = \inf_{t\in R^1} F_i^-$ and a bounded set $A_t \in C_\beta \times R^1$ plays the role of the attractor A.*

Using the auxiliary systems (4.4), we compose the comparison systems

$$\dot{\Theta}_i = F_i^{\pm}(\Theta_i) = \Delta_i - KR^{\pm}\sin\frac{\Theta_i}{2}, \quad i = \overline{1,N},$$
$$R^{+} = \begin{cases} 2 & \text{for } \Theta_i \in [-\alpha, 0), \\ 2\cos\frac{3\alpha}{2} & \text{for } \Theta_i \in [0, \alpha], \end{cases} \tag{4.11}$$
$$R^{-} = \begin{cases} 2\cos\frac{3\alpha}{2} & \text{for } \Theta_i \in [-\alpha, 0), \\ 2 & \text{for } \Theta_i \in [0, \alpha]. \end{cases}$$

From the comparison principle we derive the following sufficient condition for the Kuramoto oscillators' phase synchronization.

Theorem 2. *In the parameter range*

$$|\Delta_i| < 2K\sin\alpha\Big(\cos\alpha - \frac{1}{2}\Big) \tag{4.12}$$

the system (2.1) *has an attractor* $A \subset C$ *corresponding to the phase synchronization with the phase mismatch equal to* α.

Proof. The comparison system (4.11) has the stable equilibrium points

$$\beta_i^{-(+)} = 2\arcsin\Delta_i(2K)^{-1}, \quad \beta_i^{+(-)} = 2\arcsin\Delta_i\Big(2K\cos\frac{3\alpha}{2}\Big)^{-1} \tag{4.13}$$

for $\Delta_i > 0$ ($\Delta_i < 0$, respectively), $i = 1, \ldots, N$. Then the range of the frequency mismatch Δ_i is defined by the condition $-\alpha < \beta_i^{-} < \beta_i^{+} < \alpha$, i.e., $C_\beta \subset C$. From the critical values $\beta_i^{-} = -\alpha$, $\beta_i^{+} = \alpha$ we obtain the band $|\Delta_i| < 2K\cos\frac{3\alpha}{2}\sin\frac{\alpha}{2}$ equivalent to (4.12). □

It is easy to verify that the time dependence of mismatch Δ_i does not affect the synchronization range when $\Delta_i(t)$ satisfies (4.12) for any $t > 0$, i.e., the synchronization mode is insensitive to bounded perturbations.

5. CONDITION FOR THE ASYNCHRONOUS MODE OF THE KURAMOTO OSCILLATORS

The asynchrony of oscillators implies the mean increase(decrease) of all phase differences Θ_i. From the system (2.10) we obtain a "rough" sufficient condition for such a mode.

Theorem 3. *In the parameter range*

$$|\Delta_i| > 2K$$

all trajectories of the system (2.10) *rotate and all* N *oscillators are asynchronous.*

Indeed, in this case $\dot{\Theta}_i > 0\,(\dot{\Theta}_i < 0), i = \overline{1,N}$ due to Eqs. (2.10).

6. NUMERICAL VALIDATION

In this section we provide the results of numerical simulation of the Kuramoto ensemble and compare them against theoretical estimates obtained previously. Various values of the number of oscillators N and two kinds of individual frequency distributions were considered throughout the simulations. The first distribution is linear of the kind $\omega_i = \omega_0 + i * \Delta/N$, $i = \overline{1,N}$. The second one is a random uniform distribution in the interval $[\omega_0, \omega_0 + \Delta]$.

The condition (4.12) gives the relation between the synchronization phase angle α, coupling K and frequency mismatch Δ. So, in the first numerical experiment we compare the dependency of α on K for fixed $\omega_0 = 1$, $\Delta = 1$. The size of the ensemble $N = 100$. The results are shown in Fig. 1. The red curve with circles is obtained numerically, while solid blue is the theoretical approximation (4.12). First of all, note that for small K there is no synchronization in the system.

Hence, even the numerical curve breaks here. The corresponding distribution of oscillators over the phase circle is shown in the inset for $K = 0.1$. The phases are distributed almost uniformly over the circle, although some clusters already start to establish themselves, since the coupling is nonzero. Next, for large values of K the locking angle goes down as expected and the almost exact correspondence of simulation and theory is observed. However, if we start decreasing K from that point, then as α increases, the divergence of theory and experiment happens. This is due to the fact that all the estimations made are valid for $\alpha < \pi/3$ and the condition (4.12) has a singularity at this point (the right-hand side vanishes, which demands infinitely large K in order for the inequality to hold).

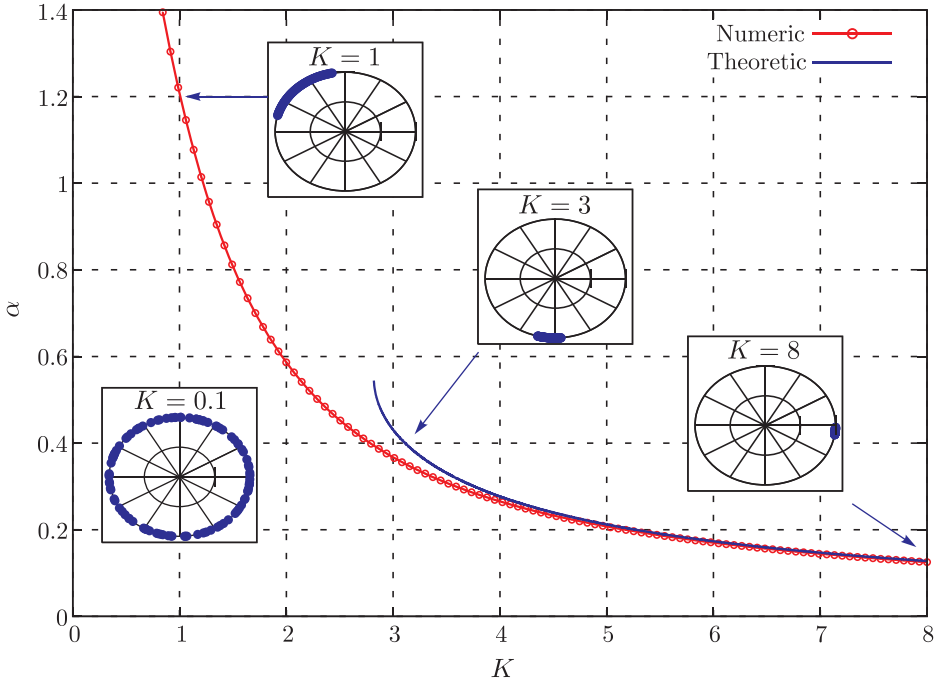

Fig. 1. The dependency of the synchronization phase locking angle α on K. The red-circle line is the numerical result; the blue curve is the theoretical approximation. The insets represent the distribution of phases over the unit circle for specified values of $K = 0.1, 1, 3, 8$.

Now let us compare the synchronization region provided by (4.12) with the exact one obtained numerically. We consider $N = 10, 100$ and for each experiment we fix α at some value: $\pi/6$, $\pi/12$. Both linear and random distributions are tested. In each experiment for fixed α we vary Δ ($\omega_0 = 1$) and for all of its values we find the K sufficient to provide synchronization in the ensemble within the angle α. The results are shown in Fig. 2. The two red lines with start markers represent the synchronization boundary obtained numerically for $\alpha = \pi/6$, $\pi/12$ and the linear frequency distribution. The boundaries are linear and the one for $\alpha = \pi/12$ has larger K. The curves with circle and rectangle markers correspond to the upper and lower theoretical margins, respectively (blue for $\alpha = \pi/6$ and red for $\alpha = \pi/12$). One can observe that the numerical boundary is always inside the two theoretical margins. Moreover, the gap is smaller for larger α and smaller Δ. The overall correspondence between the numerical data and theory is quite good. There are two more data plots in Fig. 2 with up- and down-triangle markers (no line). These represent the experiments with random delta distribution for $N = 10$, $\alpha = \pi/12$ and $N = 100$, $\alpha = \pi/6$. It is clearly seen that they exactly match the red lines, which means that there is no dependency at all on N and the distribution type. What matters is α. Theoretical approximation (4.12) does not have any dependency on N and frequency distribution either.

Finally, we find how the coupling strength K depends on α. The numerical result is shown in Fig. 3 with a magenta curve with square markers. The corresponding lower and upper theoretical limits on K are plotted as black-star and green-circle curves, respectively. One can see that the numerical result and both theoretical limits tend to meet each other for low alphas, while the

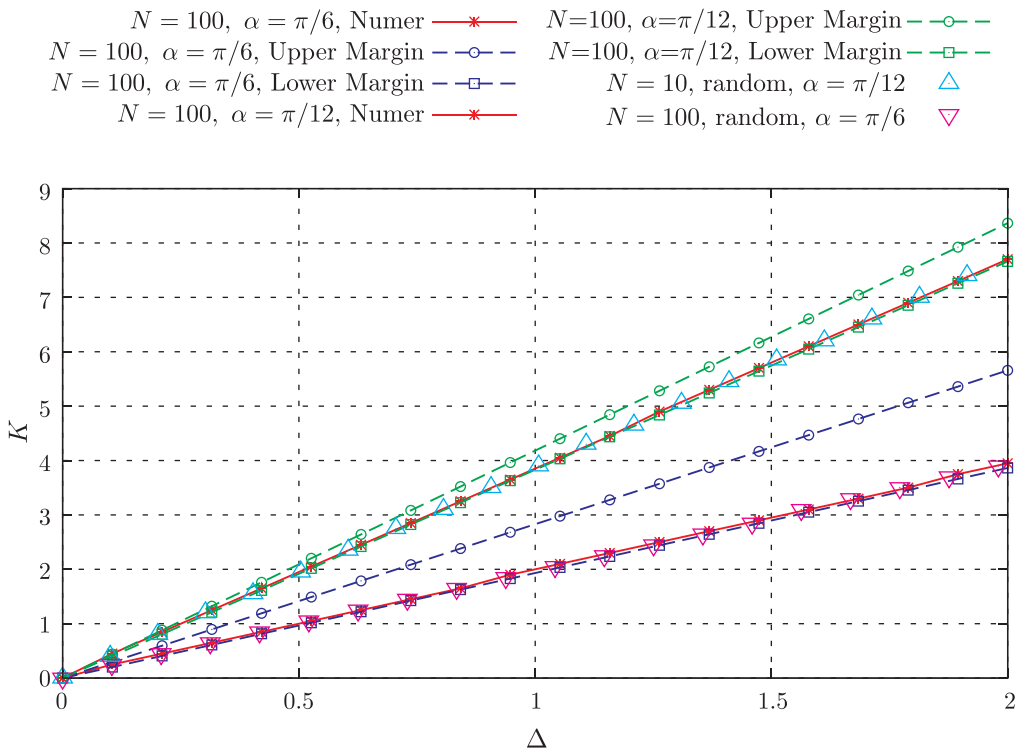

Fig. 2. Numerically obtained synchronization regions for $\alpha = \pi/6,\ \pi/12$ as well as theoretical upper and lower bounds on critical K. See the text for details.

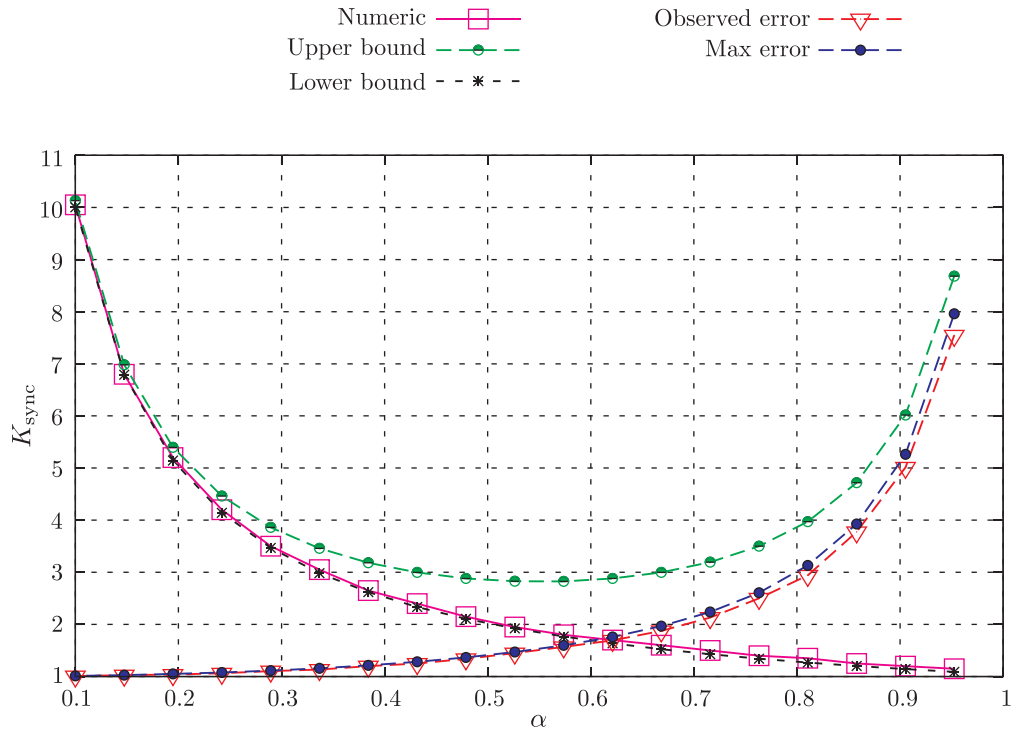

Fig. 3. The dependency of the critical coupling K on α: the magenta squares represent numerical data; black stars and green circles are the theoretical lower and upper bounds, respectively. The red triangles represent the observed relative error, the blue circles correspond to the maximum possible error estimated theoretically. See the text for details.

difference becomes more and more significant as α approaches $\pi/3$. The relative observed error between the theoretical synchronization limit (which is its upper bound) and the experimental critical K is shown as a red-triangle line. The error is almost equal to 1 for small alpha (which implies exactness of the theoretical approximation there) and grows for larger alpha. We can provide a theoretical estimate on this relative error: $e = \cos(\alpha/2)/\cos(3\alpha/2)$ (this follows from the right-hand side of the comparison systems). It is shown as a blue-circle curve in Fig. 3. Firstly, the curve in the graph is always higher than that of the observed error, which means that the estimate is correct. Secondly, it is remarkable that this relative error depends on α only and does not depend even on Δ. This means that the theoretical approximation (4.12) can be used for any frequency distribution with the same relative error.

This result concludes the numerical validation section. We showed here that the main result of the paper, which is the theoretical condition (4.12), does hold for different N, Δ, α. It approximates reality almost exactly for small α, while for larger values it has a relative error that depends on α only. We also gave an estimate on this error.

7. SUFFICIENT CONDITIONS FOR THE CHIMERA STATES

We introduce two parts of oscillators: first N_s, and second N_a, $N = N_s + N_a$, and the parameter $\mu = \frac{N_a}{N}$ indicating a fraction of the second oscillators in the ensemble. Let us rewrite Eqs. (2.10) for each part of oscillators in the following form:

$$\begin{aligned}
\dot\Theta_i &= \tilde\Delta_i - 2K(1-\mu)\left[\frac{1}{N_s}\sum_{j=1}^{N_s}\cos\Big(\frac{\Theta_i}{2}-\Theta_j\Big)\right]\sin\frac{\Theta_i}{2},\\
\tilde\Delta_i &= \Delta_i - 2K\mu\left[\frac{1}{N_a}\sum_{k=1}^{N_a}\cos\Big(\frac{\Theta_i}{2}-\Theta_{N_s+k}\Big)\right]\sin\frac{\Theta_i}{2}, \quad i=1,\dots,N_s
\end{aligned} \tag{7.1}$$

and

$$\dot\Theta_i = \Delta_i - 2K\left[\frac{1}{N}\sum_{j=1}^{N}\cos\Big(\frac{\Theta_i}{2}-\Theta_j\Big)\right]\sin\frac{\Theta_i}{2}, \quad i=N_s+1,\dots,N. \tag{7.2}$$

Due to Theorem 3 the second part of oscillators is asynchronous with respect to the leading oscillator, regardless of the dynamics of the first part of oscillators, under the condition

$$|\Delta_i| > 2K, \quad i = \overline{N_s+1, N}. \tag{7.3}$$

Now we obtain a condition for the first part of oscillators to be synchronous with respect to the leading oscillator. In order to use the comparison principle for the subsystem (7.1), we introduce the bounds of the terms $\tilde\Delta$.

$$\Delta_i - 2K\mu < \tilde\Delta_i < \Delta_i + 2K\mu, \quad i=1,\dots,N_s. \tag{7.4}$$

Note that these bounds are compatible with (7.3).

Theorem 4. *Let both the conditions*

$$|\Delta_i| < 2K\Big((1-\mu)\cos\frac{3\alpha}{2}\sin\frac{\alpha}{2} - \mu\Big), \quad i=1,\dots,N_s \tag{7.5}$$

for the first part of oscillators and the conditions (7.3) *for the second part of oscillators hold. Then the system* (2.1) *has a chimera state such that first N_s oscillators* (*including the leading one*) *are phase-synchronized, and all the remaining N_a oscillators are asynchronous with respect to the first N_s oscillators.*

Proof. Similarly to Theorem 2, we conclude that if the bounds (7.4) are located within the range (4.12) for $i = 1,\dots,N_s$, i.e., if the following inequalities hold:

$$-2K\sin\frac{\alpha}{2}\cos\frac{3\alpha}{2} < \Delta_i - 2K\mu, \quad 2K\sin\frac{\alpha}{2}\cos\frac{3\alpha}{2} > \Delta_i + 2K\mu, \tag{7.6}$$

the first part of oscillators is in phase synchronous state with the leading oscillator. The conditions (7.5) follow from (7.6). □

7.1. Numerical Proof

In this section we verify the conditions of Theorem 4 by direct simulation of an ensemble of $N = 100$ oscillators. We chose $\mu = 0.1$, i.e., there should be 90 oscillators comprising synchronous clusters as well as 10 asynchronously rotating units alltogether forming a chimera state. The frequencies of the ensemble are chosen in the following way: (i) the first 90 frequencies are drawn from uniform random distribution with $\omega_i \in [1 : 1 + \Delta_1]$; (ii) the frequencies of the last 10 oscillators are $\omega_i = f_i + \xi$, where f_i are chosen randomly again from $[1 : 1 + \Delta_2]$ and ξ is the frequency gap between the first 90 and the last 10 oscillators. With $K = 4, \Delta_1 = 1, \Delta_2 = 2, \xi = 8$ the conditions (7.3) and (7.5) are met and one observes the chimera state in the system according to the theory. Figure 4 illustrates the chimera state for this parameter set. Firstly, we calculated the phase differences $\delta\varphi_i(t) = \varphi_i(t) - \varphi_0(t)$ and then those values are vizualized at the time moments $t_n = T_0 * n$ where T_o is the rotation period of the first oscillator. This strobe plot is shown in Fig. 4 using blue circles and left axes. One can see that while all $\delta\varphi_i$ for $i < 90$ lie inside a fixed angle implying phase synchronization of those 90 units, other 10 values occupy the whole interval $[0 : 2\pi]$, which means that those oscillators rotate with respect to the first oscillator. The individual frequencies of the oscillators are shown in the same figure with red filled circles using the right axes. Those frequencies also prove the existence of the chimera state here.

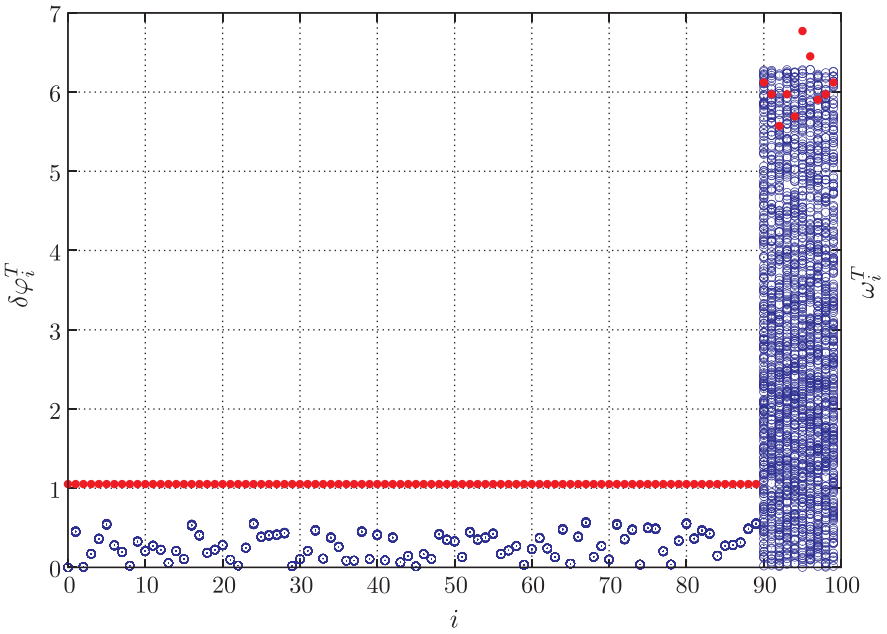

Fig. 4. Chimera state in the Kuramoto system for $N = 100$, $\mu = 0.1$, $K = 4$, $\Delta_1 = 1$, $\Delta_2 = 2$, $\xi = 8$. The blue empty circles (left axes) represent a strobe plot of the chimera state and the red filled circles correspond to the oscillators' frequencies (see the text for details).

However, in the same system other regimes may be observed for different values of Δ_2 and K. For example, increasing K may lead to global synchronization in the system, while decreasing Δ_2 may result in the synchrony inside the last 10 oscillators, thus providing a 2-cluster synchronous regime. So, a diagram of the dynamical regimes on the parameter plane Δ_2, K was calculated in order to analyze possible transitions between the different states. The diagram is shown in Fig. 5. Four main dynamical regimes are observed: GS — global synchronization, AS — global asynchrony; 2C — two-cluster regime; CH — chimera state. The frequency distributions for 4 different (Δ_2, K) points (denoted in the plot by (a), (b), (c), (d)) are shown in Fig. 5 (a, b, c, d, respectively). One can conclude from the diagram that there are 2 different scenarios for transition to the chimera state. The first one is realized when Δ_2 is fixed and is larger than some critical value, while K is being increased. In this case the transition has the form AS→CH. Further increase of K in this case gives: CH→2C→GS. An alternative scenario for the chimera state onset is observed when K is fixed and Δ_2 is being increased. Depending on K, two transitions are observed: GS→2C→CH and 2C→CH.

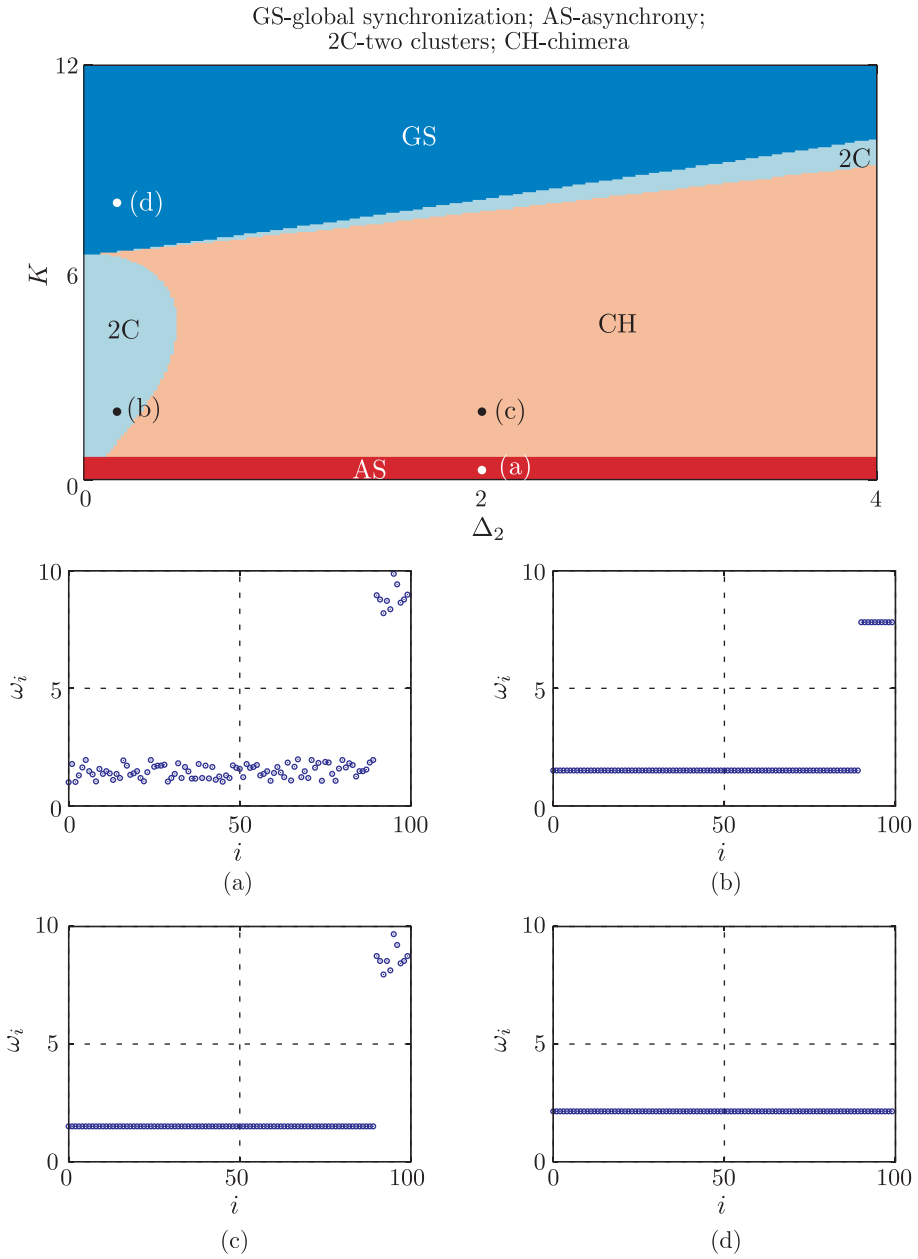

Fig. 5. The Δ_2, K diagram of dynamical regimes in the Kuramoto system with $N = 100, \mu = 0.1, \Delta_1 = 1$, $\xi = 8$. (a) asynchronous state (b) two synchronous clusters (c) synchronous cluster and chimera state (d) global synchronous state.

In both cases the chimera state sets in after the 2-cluster synchronous regime. Interestingly, the region occupied by the AS regime does not depend on Δ_2. In other words, we cannot observe synchronization in the last 10 oscillators, while the first 90 are not synchronized (if we could do it, this would be a chimera with 10 synchronized and 90 rotating units). The unexpected fact that this is true even for very small Δ_2 including $\Delta_2 = 0$, i.e., when the last 10 oscillators are identical. This is because for such small K the 90 oscillators desynchronize the remaining 10 even when the latter are identical.

8. CONCLUSIONS

In this paper we have studied the global synchronization mode of the finite-dimensional Kuramoto model. For this purpose we presented a normal form obtained by eliminating the uncertainty in the original Kuramoto model. We proposed a simple method of comparison, which

allowed us to obtain an explicit estimate of the phase synchronization range. This estimate is valid both for constant and time varying frequency mismatch. Detailed numerical simulations confirmed all theoretical results. Cluster synchronization and chimera states were found. We hope that this paper provides new insights into cooperative dynamics in oscillatory networks.

ACKNOWLEDGMENTS

This research (Sections 1—3) was supported by the Russian Science Foundation (Project 14-12-00811), by the grant N 14.B25.31.0008 between the Ministry of Education of the Russian Federation and the Lobachevsky State University of Nizhny Novgorod (Section 4) and by the RFBR grant 15-01-08776 (Section 5).

REFERENCES

1. Winfree, A. T., Biolopgical Rhythms and the Behavior of Coupled Oscillators, *J. Theoret. Biol.,* 1967, vol. 16, pp. 15–42.
2. Kuramoto, Y., *Chemical Oscillations, Waves and Turbulence,* Berlin: Springer, 1984.
3. Kuramoto, Y., Self-Entrainment of a Population of Coupled Non-Linear Oscillators, in *Internat. Symp. on Mathematical Problems in Theoretical Physics (Kyoto University, Kyoto (Japan), January 23–29, 1975),* H. Araki (Ed.), Lect. Notes Phys., vol. 39, New York: Springer, 1975, pp. 420–422.
4. Michaels, D. C., Matyas, E. P., and Jalife, J., Mechanisms of Sinoatrial Pacemaker Synchronization: A New Hypothesis, *Circ. Res.,* 1987, vol. 61, no. 5, pp. 704–714.
5. Brown, E., Holmes, P., and Moehlis, J., Globally Coupled Oscillator Networks, in *Perspectives and Problems in Nonlinear Science: A Celebratory Volume in Honor of Larry Sirovich,* E. Kaplan, J. E. Marsden, K. R. Sreenivasan (Eds.), New York: Springer, 2003, pp. 183–215.
6. Kopell, N. and Ermentrout, G. B., Coupled Oscillators and the Design of Central Pattern Generators, *Math. Biosci.,* 1988, vol. 90, pp. 87–109.
7. Wiesenfeldt, K., Colet, P., and Strogatz, S., Frequency Locking in Josephson Junction Arrays: Connection with the Kuramoto Model, *Phys. Rev. E,* 1998, vol. 57, pp. 1563–1567.
8. Neda, Z., Ravasz, E., Vicsek, T., Brecht, Y., Barabasi, A.-L., Physics of the Rhythmic Applause, *Phys. Rev. E,* 2000, vol. 61, pp. 6987–6992.
9. Strogatz, S. H., Abrams, D. M., McRobie, A., Eckhardt, B., Ott, E., Theoretical Mechanics: Crowd Synchrony on the Millenium Bridge, *Nature,* 2005, vol. 438(70640), pp. 43–44.
10. Kozyrev, G., Vladimirov, A. G., and Mandel, P., Global Coupling with the Time Delay in an Array of Semiconductor Lasers, *Phys. Rev. Lett.,* 2000, vol. 85, no. 18, pp. 3809–3812.
11. York, R. A. and Compton, R. C., Quasi-Optical Power Combining Using Mutually Synchronized Oscillator Arrays, *IEEE Trans. Automat. Contr.,* 2012, vol. 57, no. 4, pp. 920–935.
12. Dorfler, F. and Bullo, F., Synchronization in Complex Networks of Phase Oscillators: A Survey, *Automatica,* 2014, vol. 50, no. 6, pp. 1539–1564.
13. Acebron, J. A., Bonilla, L. L., Vicente, C. J. P., Ritort, F., and Spigler, R., The Kuramoto Model: A Simple Paradigm for Synchronization Phenomena, *Rev. Modern Phys.,* 2005, vol. 77, no. 1, pp. 137–185.
14. Gupta, Sh., Campa, A., and Ruffo, S., Kuramoto Model of Synchronization: Equilibrium and Nonequilibrium Aspects, *J. Stat. Mech. Theory Exp.,* 2014, no. 8, R08001, 61 pp.
15. Aeyels, D. and Rogge, J. A., Existence of Partial Entrainment and Stability of Phase Locking Behavior of Coupled Oscillators, *Progr. Theor. Exp. Phys.,* 2004, vol. 112, no. 6, pp. 921–942.
16. Mirollo, R. E. and Strogatz, S. H., The Spectrum of the Partially Locked State of the Kuramoto Model of Coupled Oscillators, *Phys. D,* 2005, vol. 205, nos. 1–4, pp. 249–266.
17. Verwoerd, M. and Mason, O., Global Phase-Locking in Finite Populations of Phase-Coupled Oscillators, *SIAM J. Appl. Dyn. Syst.,* 2008, vol. 7, no. 1, pp. 134–160.
18. Jadbabaie, A., Motee, N., and Barahona, N., On the Stability of the Kuramoto Model of Coupled Oscillators, in *Proc. of the American Control Conference (Boston, Mass., June 30 2004–July 2, 2004): Vol. 5,* pp. 4296–4301.